Water Practice & Technology Vol 16 No 3
doi: 10.2166/wpt.2021.033

Modeling climate change impacts on crop water demand, middle Awash River basin, case study of Berehet woreda

Negash Tessema Roba[a,*], Asfaw Kebede Kassa[b] and Dame Yadeta Geleta[c]

[a] Water Resources and Irrigation Engineering Department, Haramaya Institute of Technology, Haramaya University, P.O. Box 138, Dire Dawa, Ethiopia

[b] Hydraulic and Water Resources Engineering Department, Haramaya Institute of Technology, Haramaya University, P.O. Box 138, Dire Dawa, Ethiopia

[c] Natural Resources Management Department, College of Dry Land Agriculture, Samara University, P.O. Box 132, Samara, Ethiopia

*Corresponding author. E-mail: sifankiya53@gmail.com

Abstract

Climate change mainly affects crops via impacting evapotranspiration. This study quantifies climate change impacts on evapotranspiration, crop water requirement, and irrigation water demand. Seventeen GCMs from the *MarkSim-GCM* were used for RCP 4.5 and 8.5 scenarios for future projection. A soil sample was collected from 15 points from the maize production area. Based on USDA soil textural classification, the soil is classified as silt loam (higher class), clay loam (middle class), and clay loam (lower class). The crop growing season onset and offset were determined using the Markov chain model and compared with the farmer's indigenous experience. The main rainy season (*Kiremt*) starts during the 1st meteorological decade of June for baseline period and 2nd decade to 3rd decade of June for both RCP 4.5 and RCP 8.5 of near (2020s) and mid (2050s) future period. The offset date is in the range of 270 (base period), RCP 4.5 (278, 284), and RCP 8.5 (281, 274) DOY for baseline, near, and mid future. The rainfall and temperature change show an increasing pattern from the base period under both scenarios. Furthermore, the reference evapotranspiration (ETo) estimating model was developed using multiple variable regression and used for a future period in this study. In the base period, ETo increases from 33.4 mm/dec in the 1st decade of July to the peak value of 52.1 mm/dec in the 3rd decade of May. Under RCP8 .5, the 2nd decade of August ET_O is minimal (44.3 mm/dec), while in 1st decade of April ET_O was maximum (75.3 mm/dec) and raise from 44.3 mm/dec in the 2nd decade of August to the peak value of 75.3 mm/dec in the 1st decade of April. Under RCP 4.5, ET_O raises from 33 mm/dec in the 1st decade of Dec to the peak value of 48 mm/dec in the 3rd decade of May. ETo shows an increasing trend from the base period under both scenarios. During the base period, a maize variety with a growing period of 110 days required 403.2 mm depth of water, while 67 mm is required as supplementary irrigation. Crop water and irrigation requirements of the maize variety with a growing period of 110 days are predicted to be 436.1 and 445.1 mm water during the 2020 and 2050 s for RCP 4.5, while 101.8 to 63.7 mm depth of water as supplementary irrigation respectively and 441.3 and 447.3 mm of water during 2020 and 2050 s of the future period for RCP 8.5, while 142.9 to 134.0 mm required as supplementary irrigation for both periods of RCP 8.5 scenarios. Crop water need will increase by 8.16 and 10.39% for RCP 4.5 and by 9.45 and 10.94% for RCP 8.5 of the 2020 and 2050 s respectively. In this study, a new ETO model is developed using a multiple variable linear regression model and its degree of the fitting is statistically tested and Kc is adjusted for the local climate, and hence, can be used in future irrigation and related studies. Generally, decision-makers, farmers, Irrigation engineers, and other stakeholders can use the results of this study in irrigation design, monitoring, scheduling, and other related activities.

Water Practice & Technology Vol 16 No 3
doi: 10.2166/wpt.2021.033

Key words: climate change, crop water, evapotranspiration, irrigation, middle Awash basin

Highlights

- The crop growing season onset and offset were determined using the Markov chain model and compared with the farmer's indigenous experience.
- The rainfall and temperature change show an increasing pattern from the base period under both RCP 4.5 and RCP 8.5 scenarios.
- Reference evapotranspiration shows an increasing trend from the base period (1984-2013) under both RCP 4.5 and RCP 8.5 scenarios.
- Crop water need will increase by 8.16 and 10.39% for RCP 4.5 and by 9.45 and 10.94% for RCP 8.5 of the 2020s and 2050s respectively.
- A new reference evapotranspiration model is developed using a multiple variable linear regression model, its degree of the fitting is statistically tested and Kc is adjusted for the local climate; hence, it can be used in future irrigation and related studies.

Graphical Abstract

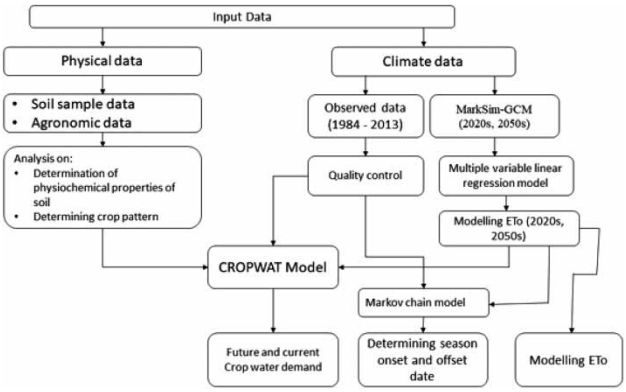

INTRODUCTION

Global food security is mainly being challenged by climate unpredictability in the world. Climate change refers to the increase in earth temperature due to the release of greenhouse gases into the earth's atmosphere (IPCC 2007). It remains a challenge for scholars to quantify its local impact due to the global scale of its impact. The climate change impact on crops can be impressive, due to fluctuations in the amount of CO_2 available for photosynthesis. Additionally, climatic factors such as temperature, precipitation, moisture, and pressure influence the plants' growth, either alone or in assistance with other factors (Cutforth *et al.* 2007).

Climate change leads to water scarcity and worsens desertification (Saad *et al.* 2011; OECD 2013). It also affects crop evapotranspiration and thus the irrigation water requirement (Osborne *et al.* 2000; Quiroga & Iglesias 2009). Crop evapotranspiration plays a key role in the designation and management of crop irrigation schedules (Djaman *et al.* 2018). Therefore, determining the irrigation water requirement of crops is very crucial for optimal irrigation scheduling. One of the most widely used means to determine crop water use is demand-based judgment (Ko *et al.* 2009; Ghamarnia *et al.* 2013). This approach uses the estimated ET and a crop-specific coefficient (Kc) to approximate the crop water use (Allen *et al.* 1998).

Water Practice & Technology Vol 16 No 3
doi: 10.2166/wpt.2021.033

Globally, the population inhabiting dry lands exceeds two billion, which constitutes approximately 40% of the world's population (White & Nackoney 2003). In dryland regions, cereals are the mainly grown crops on which life depends (LADA 2008). Whereas, agricultural productivity in such areas is vitally dependent on water availability during the crop production season (Wang *et al.* 2016). Severe droughts and significant losses of yield in the arid and semi-arid zones are due to the rising temperature (Andreadis & Letten Maier 2006; Yadeta *et al.* 2020a). Similarly, in the middle Awash River basin of Ethiopia, the impacts of climate change are worsening crop production via increasing evapotranspiration losses (Yadeta *et al.* 2020b).

Thus, to bring sustainable food security in the area, drylands need to be managed precisely (UNEP 2000). To do so, promising measurements and predictions have to be accessible to safeguard water resources and agricultural sectors in drylands (Gan 2000). Ethiopia in general and the middle Awash basin, in particular, are susceptible to the impacts of climate change and variability (Tessema *et al.* 2020; Yadeta *et al.* 2020a). The higher temperature resulting from climate change will induce higher evapotranspiration (Yadeta *et al.* 2020b), which in turn affects the hydrological systems and agriculture. Investigation of climate change impacts on several sectors, particularly agriculture, is very core to the decision-makers; however, it is not well done yet in most developing countries like Ethiopia. Particularly in the middle Awash River basin, even though the impacts of climate change and variability are very devastating in the area, the study of climate change impacts on crops, soil moisture, and irrigation work through water stress is not yet investigated. Thus, estimating crop water and irrigation requirements for a proposed cropping pattern is an essential part of the planning and design of an irrigation system and it is important to convey the policy for water resources' optimal allocation along with decision-making in irrigation systems' operation and management.

Moreover, understanding the possible impacts of climate change is incredibly imperative in developing both adaptation strategies and actions to reduce climate change risks. Regrettably, the inadequacy in the information about the climate change impacts on crops reduces the ability of policy-makers to adjust their plans to cope with the future. In line with this, adaptation to climate change has received more attention compared with mitigation. Parry *et al.* (1998) indicated that adaptation is more intricate than mitigation, emission sources are relatively few, but the array of adaptation is enormous, yet to ignore adaptation is both impractical and dangerous.

Adaptation refers to efforts to reduce the system's vulnerabilities to climate change impacts. According to IPCC (2007), adaptation is concerned with responses to both the negative and positive effects of climate change. A wide range of responses can be implemented by policy decisions at the regional or national level. These adjustments are adaptation strategies (Carter 1996).

At the farm level, agricultural adaptation to climate change depends on the technological potential, such as different varieties of crops, irrigation technologies, changing sowing dates, and changing irrigation schedules. But, in the study area, such adaptation strategies are not practiced yet. On the other hand, the ability of farmers to notice climate change and carry out any necessary actions will be reflected in achieving higher crop water productivity. Assessment of climate variability impact on agriculture at the local level has an enormous advantage in Ethiopia and crop water use also needs to be accurately predicted by correctly predicting evapotranspiration and the extraction of soil water by plant roots (Richter & Semenov 2005). Therefore, this study models the impacts of climate change evapotranspiration, crop water requirement, and irrigation water demand in the middle Awash River basin of Ethiopia.

The study is structured as follows. After this introduction, the following section presents the response types to observed meteorological and future scenario weather generations considered in the present assessment. As physical data (soil sample and agronomic) is determined and available, the emphasis is placed on the methods to integrate this information into a global soil and crop water modeling framework. ETo and season onset and offset were determined using the Markov chain and multiple variable linear regression model respectively. The subsequent section compares the aggregated yield of ETo, season onset and offset and crop water demand under climate changes.

Water Practice & Technology Vol 16 No 3
doi: 10.2166/wpt.2021.033

The main drivers of changes in crop water demand are also explored through a decomposition analysis and ETo is modeling for both scenarios. The significance of the results is then discussed. The final section concludes and the limitations of the current study are set out.

RESEARCH METHODOLOGY

Description of the study area

In the Kesem sub-basin of the middle Awash River basin, Berehet is located in the range of 39°59′E to 8°55′N in the Eastern part of Ethiopia and its area coverage is about 997 km^2 (Figure 1). It is surrounded by mountains and plateaus in its northern direction and is at a distance of 268 km from the Ethiopian capital city Addis Ababa. In administrative terms, the woreda is bordered on the south by the Germama River, which separates it from Menjarna Shenkora, to the west by Hagere Mariamna Kesem, in the north by Asagirt, and with the Afar Region to the east. The climate system of the area is described as semi-arid to sub-humid in the north and northwest; but the north and northeast, which covers the majority of the area, falls in the semi-arid climate, hence it receives a mean annual rainfall of 995 and 534 mm. The rural economy of the people in the Berehet woreda is based on both agricultural production and livestock rearing.

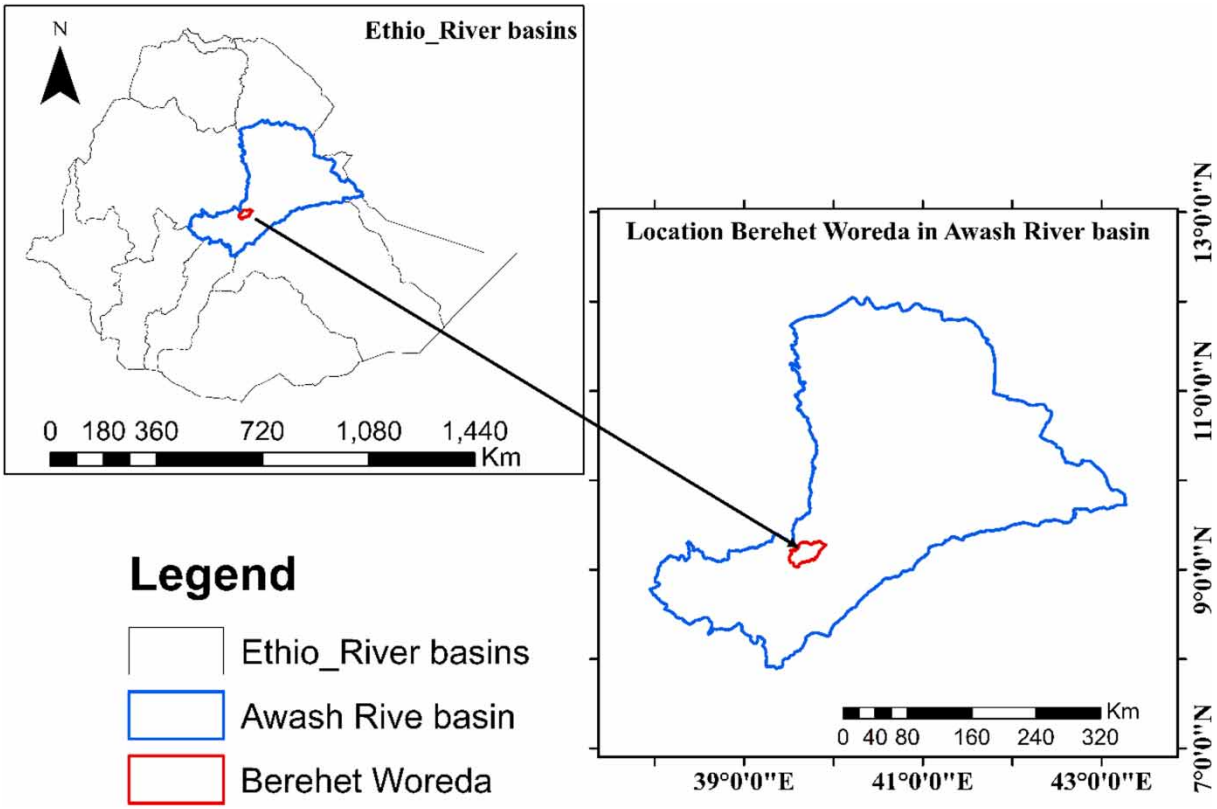

Figure 1 | Location map of the study area.

Primary data collection

Field survey and farmers experience

A reconnaissance survey was conducted to visualize the nature of possible variations on the topography and soil of the study area to identify sampling locations (points) to ease the collection of soil

Water Practice & Technology Vol 16 No 3
doi: 10.2166/wpt.2021.033

samples just for the sake of describing the soil and to scientifically compile and relate farmer's experience with the existing study's results.

Soil sampling and analysis

Soil sampling was undertaken for the Berehet woreda of the maize production area in the middle Awash basin. Thus, a total of 15 sampling points covering all selected areas of maize production land types were used. During survey work, maize-producing areas were pre-defined and the locations were collected. Based on the complexity of topography and heterogeneity of the soil type for each sampling point, 5 to 10 composite subsamples were taken from three classes by making a zigzag shape. A soil auger was used for collecting disturbed soil samples and then composited. Soil samples were taken at three depths (0–30, 30–60, and 60–90 cm).

The soil auger and other sampling tools were cleaned before taking the next sample to lessen the cross-sample contamination among samples. After processing (drying, grinding, and sieving), the soil was analyzed for soil physicochemical properties following the standard procedure compiled by Sahlemedin & Taye (2000). The analyses were conducted at Werer Agricultural Research Center soil laboratory.

Determination of soil physical properties

Soil physical parameters like soil texture, bulk density (P_d), field capacity (FC), permanent wilting point (PWP), available water holding capacity (AWHC), and water infiltration rate were determined using appropriate procedures and methods amassed by Sahlemedin & Taye (2000).

The soil texture of the field was determined in the laboratory using the pipette method (Carter & Gregorich 1993). This is based on the direct sampling of the density of the solution. Soil bulk density was determined from an undisturbed soil sample taken using a core sampler of known volume (100 cm^3) that was driven into the soil of desired depth and calculated as the ratio of the oven-dry weight of soil to a known cylinder core sampler volume. Since bulk density varies considerably spatially, the measurements were taken at three different soil depths of the soil profile and 15 samples from the selected area of the district during the wet (maize production period) season. Mathematically, it is expressed as:

$$\mathrm{BD} = \frac{\mathrm{Wd}}{\mathrm{Vr}} \tag{1}$$

where, BD = bulk density, g/cm^3;
Wd = weight of oven-dry soil, g;
Vr = volume of ring, cm^3.

Soil infiltration rates were determined at three sample locations (1 subclass × 1 replication/sample), with one sample from each class. The measurement at each sample site was done in one replication using a double-ring infiltrometer.

Secondary data

Agronomic data

Crop data, which consist of the Kc values, stage days, root depth, and depletion fraction of the crop, were taken from FAO Irrigation and Drainage (FAO 2012). Information on maize varieties used by

Water Practice & Technology Vol 16 No 3
doi: 10.2166/wpt.2021.033

local farmers and planting date (onset date) was obtained during survey work from the local farmers by informal interview.

Observed meteorological data and future scenario weather generation

Thirty years of observed meteorological data of the Shola Gebeya weather station were collected from the Ethiopian National Meteorological Agency. For future period climate projection, *MarkSim_GCM* was used, which requires only geographical location (latitude and longitude) to downscale and generate daily future weather data for a given site at the locality. *MarkSim_GCM* operates with the aid of 17 climate models. Therefore, the ensemble of the 17 GCMs Atmosphere-Ocean climate models have been used for RCP 4.5 and RCP 8.5 emission scenarios for two-time slices of the future period 2020 (2014–2043) and 2050 (2044–2073). *MarkSim_GCM* was accessed via http://gismap.ciat.cgiar.org/.

Data preprocessing

To make the weather datasets acquiescent to further analyses, the missing values were patched using the first-order Markov chain model with the aid of INSTAT plus V 3.37 (Stern *et al.* 2006) while the consistency and homogeneity of rainfall were checked by the double mass curve technique (Subramanya 2008) and using XLSTAT 2019 software by Standard Normal Homogeneity test method respectively. Finally, the projected data processes were evaluated using the standard deviation (SD) and mean absolute error (MAE), where in the latter is a quantity used to measure how close simulated forecasts were to the observed data (Willmott & Kenji 2005).

Data analysis

Determination of onset and offset date of the maize growing season

In the current study, the start and end of the rainy season were determined scientifically using the Markov chain model and compared with the farmer's indigenous experiences. Accordingly, the onset of the rainy season is defined as the first occasion from the first of June that records 20 mm of rainfall amount or more over 3 days, and will not be followed by a period of more than 9 successive dry days in the next 30 days (Stern *et al.* 2003). The situations of having no dry spells of above 10 days after the start of the rainy season eliminate the possibility of a false start of the season. A period of 30 days is the average length for the initial growth stage of most crops (Allen *et al.* 2005). The end of the season is computed using first-order Markov chain modeling by considering maximum daily evapotranspiration of 5 mm and soil available water holding capacity of 100 mm. Given the above definitions, Instat statistical tool (Version 3.37) was used.

Modeling and estimation of reference evapotranspiration

Over time, several models have been developed and used for the estimation of evapotranspiration in different parts of the world. All the models have their weaknesses and strength based on the climatic conditions of the region they developed. Some of the methods use temperature data only while others use solar radiation and sunshine data only. Among all the models developed, the Penman-Monteith FAO 56 (PMF 56) is considered the standard method (Allen *et al.* 1998). This method is the most consistent estimator of evapotranspiration among all the climate-based empirical methods.

However, it is parameter rich requiring solar radiation, the sunshine duration for estimating net radiation; maximum and minimum temperature, psychrometric or relative humidity data for estimating the vapor pressure shortfall, and wind speed. But, collecting these parameters is very challenging

Water Practice & Technology Vol 16 No 3
doi: 10.2166/wpt.2021.033

due to their rare existence in many weather stations particularly in developing countries like Ethiopia. Therefore, in this study estimation of evapotranspiration followed two procedures. For the baseline period, Penman-Monteith FAO 56 (PMF 56) was used as follows:

$$\mathrm{PET} = \frac{0.408\Delta(R_n - G) + \gamma(\frac{900}{(T+273)})U_2(e_s - e_a)}{\Delta + \gamma(1 + 0.34U_2)} \tag{2}$$

where,

ETo = Reference evapotranspiration(mm/day);
Δ = Slope of the saturated vapor pressure curve (kPa °C^{-1});
R_n = Net radiation (MJ m^{-2} day^{-1});
G = Soil heat flux density (MJ m^{-2} day^{-1});
T_m = Mean air temperature (°C) at 2.0 m;
U_2 = Average wind speed at 2.0 m height (m s^{-1});
e_s = Saturation vapor pressure (kPa) at temperature Tm;
e_a = Actual vapor pressure (kPa); ($e_s - e_a$) is the vapor pressure deficit (kPa); and
γ = Psychrometric constant (kPa °C^{-1}).

This method was used with the aid of the ***CROPWAT*** software model.

However, for the future period, an empirical model was developed based on the historical climate data using multiple linear regressions with the aid of ***SPSS*** software, and used for the future reference evapotranspiration estimation. In this case, first, the climate parameters (maximum and minimum temperature, relative humidity, wind speed, solar radiation, and sunshine hours) and the ETO that is estimated using standard FAO 56 Penman-Monteith are prepared for the model development on monthly basis. Secondly, the climate parameters are considered as independent variables, and the ETO is estimated using FAO 56 Penman-Monteith as a dependent variable.

Then the climate parameters data of the study area were tested for the fittingness of a multiple linear regression model. The relation between ETO and the climate parameters was obtained and compared with a multiple linear regression model for ETO developed using the least-squares method, whose linearity was checked by residual analysis. For a multiple linear regression model, the dependent variable $\mathbf{y}$ is assumed to be a function of $\mathbf{k}$ independent variables $\mathbf{x_1}$, $\mathbf{x_2}$, $\mathbf{x_3}$ … $\mathbf{x_k}$. The general form of the equation is computed as follows:

$$\mathbf{y_i} = \mathbf{b_0} + \mathbf{b_1 x_1}, \mathbf{i} + \cdots + \mathbf{b_k x_k}, \mathbf{i} + \mathbf{e_i}, \tag{3}$$

where $\mathbf{b_0}$, $\mathbf{b_1}$, …, and $\mathbf{b_k}$ are fitting constants; $\mathbf{y_i}$, $\mathbf{x_1}$, $\mathbf{i}$, …, $\mathbf{x_k}$, $\mathbf{I}$ represent the $\mathbf{i^{th}}$ observations of each of the variables $\mathbf{y}$, $\mathbf{x_1}$, …, $\mathbf{x_k}$, respectively; $\mathbf{e_i}$ is a random error term representing the remaining effects on $\mathbf{y}$ of variables not explicitly included in the model. For simple regression models, $\mathbf{e_i}$ can be assumed to be an uncorrelated variable with zero means. The further most common technique for estimating the values of $\mathbf{b_0}$, $\mathbf{b_1}$ … and $\mathbf{b_k}$ is to employ the least-squares criterion with the minimum sum of squares of error terms (**S**); that is to find $\mathbf{b_0}$, $\mathbf{b_1}$, … and $\mathbf{b_k}$ to minimize:

$$\mathrm{S} = \sum_{i=1}^{n} (y_{iobserved} - b_0 - b_{1\,x1,\,i} - \cdots - b_{kxk,i})^2 \tag{4}$$

$$\mathrm{S} = \sum_{i=1}^{n} (y_{iobserved} - y_{icalculated})^2 \tag{5}$$

$$\mathrm{S} = \sum_{i=1}^{n} e_i^2 \tag{6}$$

Water Practice & Technology Vol 16 No 3
doi: 10.2166/wpt.2021.033

Hence, $\mathbf{b_0}$, $\mathbf{b_1}$ … and $\mathbf{b_k}$ must satisfy the following:

$$\frac{\partial \boldsymbol{S}}{\partial \boldsymbol{bj}} = 2\sum_{\boldsymbol{i}=1}^{\boldsymbol{n}} \boldsymbol{ei}\frac{\partial \boldsymbol{ei}}{\partial \boldsymbol{bj}} = 0,\ \boldsymbol{j} = 0,\ 1,\ \ldots,\ \boldsymbol{k}, \tag{7}$$

Since, ei = yi observed – yi calculated, the above equation becomes:

$$\frac{\partial \boldsymbol{S}}{\partial \boldsymbol{bj}} = -2\sum_{\boldsymbol{i}=1}^{\boldsymbol{n}} \boldsymbol{ei}\frac{\partial \boldsymbol{yi_{calculated}}}{\partial \boldsymbol{bj}} = 0,\ \boldsymbol{j} = 0,\ 1,\ \ldots,\ \boldsymbol{k}, \tag{8}$$

This is because MarkSim_GCM gives only rainfall and temperature data. Hence, in the future period climate scenarios, only the influence of temperature (Tmax and Tmin) were considered while other weather parameters (solar radiation data or sunshine duration, relative humidity data, and wind speed) were considered from the baseline period data.

Adjustment of crop data

According to WARC (2016) and experiences of local farmers, the dominated and recommended maize varieties in the middle Awash basin is Melkassa Hybrid two (MB2). The crop data taken from (FAO56) were adjusted to the local condition of the study area. Depletion fraction was affected by ET_O (Smith *et al.* 2006) as shown below:

$$P_{adj} = P_{tab} + 0.04(5 - ET_O),\ \text{for } ET_O \approx 5,\ P_{tab} = 0.55 \tag{9}$$

where: P_{adj} – adjusted depletion fraction, P_{tab} – tabulated depletion fraction.

The K_c value highly depends on relative humidity and wind speed at the mid-stage of crop growth. Hence, when the value of relative humidity is high (RH >80%) and the wind speed is low (u < 2 m/sec) the k_c should be reduced by 0.05 and its values should be improved by 0.05 if the relative humidity is low (RH <50%) and the wind speed is high (u > 5 m/sec). The intervals out of the above situation were adjusted as:

$$K_{c\ adj} = K_{c(tab)} + (0.04(U_2{-}2) - 0.004\,(RH_{min} - 45))\,(h/3)^{0.3},\ \ h = 2m \tag{10}$$

where: $K_{c\ adj}$ – adjusted crop coefficient, $K_{c\ (tab)}$ – tabulated crop coefficient, U_2 – wind speed, h – the height of the crop, RH_{min} – minimum relative humidity.

Estimation of crop and irrigation water demand

Estimating the crop water and irrigation requirements for a proposed cropping pattern is an essential part of the planning and design of an irrigation system and important in formulating the policy for optimal allocation of water resources as well as in decision-making in the day-to-day operation and management of irrigation systems. Therefore, Crop water requirement (CWR) was estimated as:

$$CWR = K_{c\ adj} \times ETO \tag{11}$$

where:

CWR = Crop water requirement, mm/day;
$K_{c\ adj}$ = Adjusted crop coefficient (adjusted using Equation (10) above);

Water Practice & Technology Vol 16 No 3
doi: 10.2166/wpt.2021.033

ETO = evapotranspiration, mm/day (estimated using FAO 56 for base period Equation (2) and using the developed empirical model for the future period).

To estimate crop and irrigation water requirements, it is essential to estimate the effective rainfall over the cultivated area. Thus, effective rainfall (P_{eff}) was estimated using the USDA S.C (1985) method as:

$$P_{eff} = P_{month} * (125 - 0.2 * P_{month})/125, \text{ for } P_{month} <= 250\,mm \quad (12)$$

$$P_{eff} = 125 + 0.1 * P_{month}, \text{ for } P_{month} > 250\,mm \quad (13)$$

where, P_{eff} = Effective precipitation; P_{month} = mean monthly precipitation.

Irrigation requirement (IRn) is the water that must be supplied through the irrigation system to ensure that the crop receives its full crop water requirement. Therefore, Irrigation water requirement (IRn) was computed using:

$$IRn = CWR - Pe \quad (14)$$

where:

IRn = Net irrigation requirement (mm);
CWR = Crop water requirement (mm);
Pe = Effective rainfall (mm).

RESULTS AND DISCUSSION

Rainfall and temperature change

The analysis showed that there was an increment in rainfall and temperature in the district. Rainfall show the likely increase within the range of +5.7 to +9.51% and +3.45 to +6.43% for both RCP 4.5 and RCP 8.5 scenarios respectively (Figure 2). This result implies that wet condition are likely the prevailing weather of the future in the district (Kim & Yu 2012; Weller & Cai 2013). This finding is in harmony with the results of (Kim *et al.* 2008; IPCC 2013; Gebremeskel & Kebede 2017; Osima 2018; Yadeta *et al.* 2020a, 2020b; Tessema *et al.* 2020).

The minimum temperature was projected to increase by 1.04 °C to +3.02 °C and +0.03 °C to 5.13 °C under both scenarios for the 2020 and 2050 s and consistent with the result of (IPCC 2013; Tekleab *et al.* 2013; Osima 2018; Yadeta *et al.* 2020a, 2020b). Also, the maximum temperature was expected to increase in the range of +0.95 °C to +1.98 °C and +1.38 °C to +2.83 °C for the 2020 and 2050 s of both scenarios. The change in minimum temperature was faster and greater than the maximum temperature. Such change is common globally (Paeth *et al.* 2005; Gebrehiwot & van der Veen 2013; Tekleab *et al.* 2013; Osima 2018) which indicates warming nights have occurred in recent times. The occurrence of high-temperature possesses occurrence of heavy rainfall, the reason is increasing temperature creates active hydrological cycle (IPCC 2013). Likewise, increasing temperature causes high evapotranspiration and, then crop and irrigation water requirement (Yadeta *et al.* 2020b).

Onset, offset, and length of the growing period of maize

The main rainy season (Kiremt) starts during the 1st meteorological decade of June for the baseline period and 2nd decade to 3rd decade of June for both RCP 4.5 and RCP 8.5 of near (the 2020s) and mid (the 2050s) future period.

Water Practice & Technology Vol 16 No 3
doi: 10.2166/wpt.2021.033

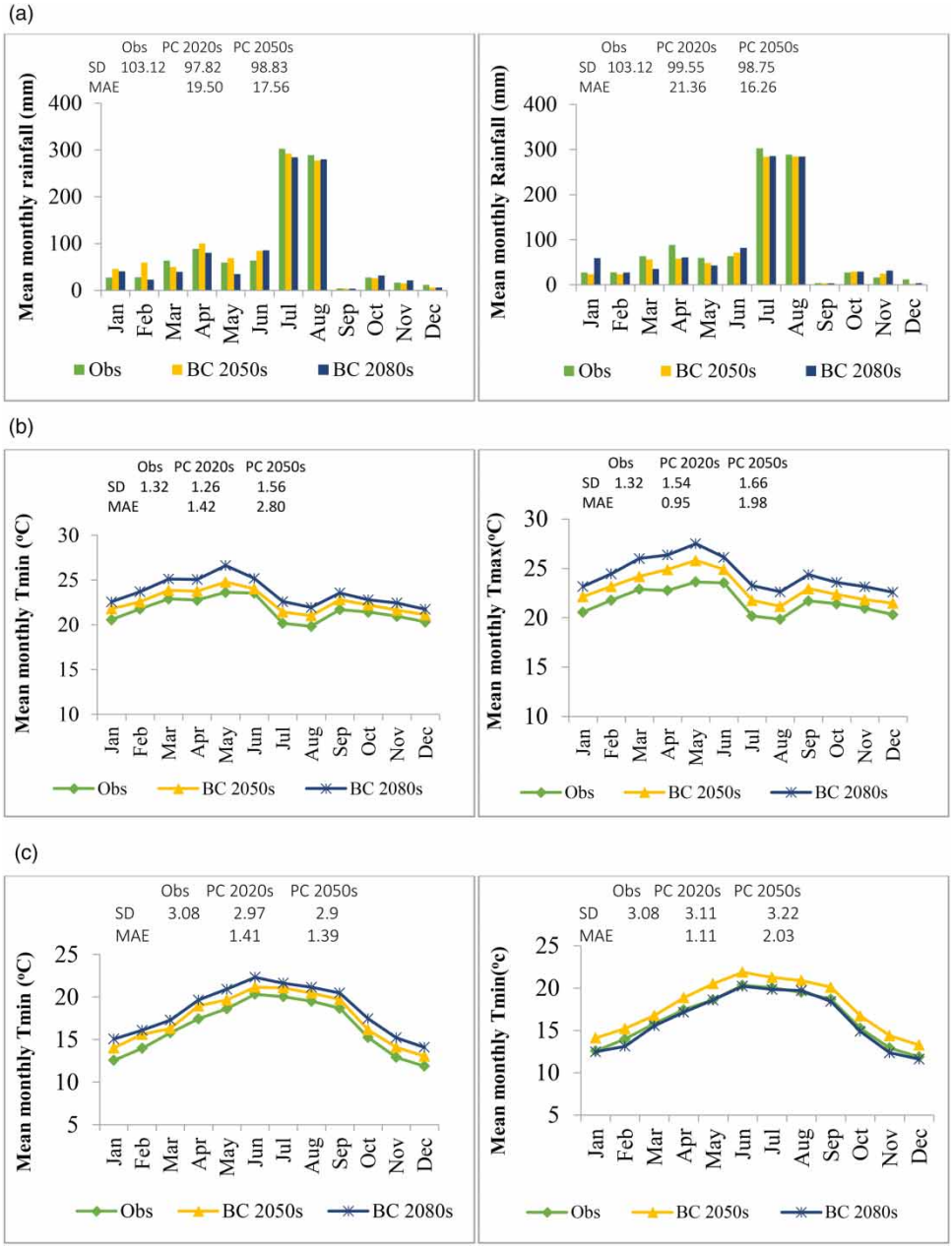

Figure 2 | Projected change in monthly rainfall (a), Tmax (b), and Tmin (c) from the base period for RCP 4.5 (left panel) and RCP8.5 (right panel) scenarios. *Note*: Obs-observed, and PC- Projected change.

The onset dates lower and upper quartile falls between 152 to 167 DOY (day of the year) for the base period and 156 to 184 DOY for the 2020 and 2050 s for both scenarios (Table 1). This implies that the chance of getting an onset date on 167 and 184 DOY is 75% and can expect the situation at 152, 156, 151, and 161 DOY for both periods (Table 1). The earliest date of onset date was 131, 136,149, and 150 DOY while the latest date was 181 (base period), RCP 4.5 (186, 196) and RCP 8.5 (209, 192) and the optimal planting date was 156 (base period), RCP 4.5 (161, 171), RCP 8.5 (168, 173) for the base period, the 2020s and 2050s.

Late onset shortens the available length of the crop growing period and the potential to satisfy the crop water requirement (Green 1966). However, the baseline and future variability of onset date showed less variability compared to LGP but highly variable than cessation date, and showed less standard deviation compared to LGP but higher than cessation. The higher standard deviation of the onset date indicates that patterns could not be easily understood and consequently, decisions

Water Practice & Technology Vol 16 No 3
doi: 10.2166/wpt.2021.033

Table 1 | Descriptive statistics of onset date (a), offset date (b), length of growing period (c)

		RCP 4.5		RCP 8.5	
(a)	Base period 1984–2013	2014–2043	2044–2073	2014–2043	2044–2073
N	30	30	30	30	30
Min	131	150	136	136	149
Q1 (25%)	152	156	151	156	161
Q2 (50%)	156	161	171	168	173
Q3 (75%)	167	169	184	178	181
Max	181	186	196	209	192
Mean	157	162	168	168	170
SD	14	10.1	17.8	17.3	13.2
CV (%)	8.9	6.2	10.6	10.3	7.7
		RCP 4.5		RCP 8.5	
(b)	Base period 1984–2013	2014–2028	2028–2043	2014–2043	2043–2073
N	30	30	30	30	30
Min	267	274	274	274	274
Q1 (25%)	267	274	274	274	274
Q2 (50%)	270	278	284	281	274
Q3 (75%)	278	291	299	287	288
Max	289	300	316	303	297
Mean	275	281	286	282	279
SD	3.86	8.9	12.8	8.2	8.1
CV (%)	1.4	3.2	4.5	2.9	2.9
		RCP 4.5		RCP 8.5	
(c)	Base period 1999–2013	2014–2043	2044–2073	2014–2043	2044–2073
N	30	30	30	30	30
Min	88	89	78	78	82
Q1 (25%)	115	113	99	100	95
Q2 (50%)	114	117	118	117	112
Q3 (75%)	111	130	134	120	124
Max	139	138	165	145	131
Mean	113	118	117	113	108
SD	13	13	22.9	16.5	14.7
CV (%)	12.4	11	19.4	14.5	13.6

N, number of data set; min; minimum value, Q1 (25%), first quartile; Q2 (50%), second quartile; Q3 (75%), third quartile; max, maximum value; SD (±); standard deviation; CV, coefficient of variation.

relating to crop planting and related activities must be made with a high level of caution. The result is similar to the study undertaken by Abiy *et al.* (2014), which stated that informed decision-making in crop planting is the essential activity in agricultural planning more importantly when aligned with characteristics of onset, offset, and LGP of the rainy season.

The offset date is in the range of 270 (base period), RCP 4.5 (278, 284), and RCP 8.5 (281, 274) DOY for baseline, near, and mid future periods respectively, as shown in Table 1. The upper quartile, lower quartile, minimum and maximum for offset date during the base period indicate that for the chance of getting 75% of the time, the end date will occur at 270 to 284 DOY. The LGP for maize production in the main rainy season ranged from 93 to 165 rainfall days for the baseline and future period

Water Practice & Technology Vol 16 No 3
doi: 10.2166/wpt.2021.033

respectively. The mean LGP of the area ranges from 113 to 118 rainfall days. This study agrees with Yadeta *et al.* (2020a).

Soil characteristics analysis

The results for the composition of clay, silt, and sand percentages are shown in Table 2. Thus, as per the USDA soil textural classification, the soil was classified as silt loam (higher class), clay loam (middle class), and clay loam (lower class) soil.

Table 2 | The average particle size distribution of five sampling points for each class of the selected area

		Particle size distribution (%)			
Class	**Soil depth (cm)**	**Clay**	**Silt**	**Sand**	**Textural class**
Higher	0–30	10.6	77.6	11.8	Silt loam
	30–60	20.4	69.2	10.4	
	60–90	22.4	67.8	9.8	
Average		17.8	71.5	10.7	
Middle	0–30	47.8	33.0	19.2	Clay loam
	30–60	33.2	42.6	24.2	
	60–90	31.2	44.6	24.2	
Average		37.4	40.1	22.5	
Lower	0–30	41.4	35.8	22.8	Clay loam
	30–60	38.4	37.0	24.6	
	60–90	39.6	35.0	25.4	
Average		39.8	35.9	24.3	

Soil bulk density of the area showed variation with the land class (Table 3) for all soil textures. It varied between 1.41 to 1.47 gm cm^{-3} and generally, the lower class soil has slightly lower bulk density than the middle and higher class, with an average bulk density of 1.42 gm cm^{-3} for clay loam texture. From higher to lower class, the soil bulk density decreases. As bulk density increases, soil pore space gets smaller, tending to increase soil compaction. The smaller the soil compaction, the greater the moisture content at field capacity and permanent wilting point in the selected area, and the reverse was true for higher soil compaction.

Table 3 | Laboratory analysis results of soil samples

Soil texture	**Soil depth (cm)**	P_d	**Mc**	**FC (%)**	**PWP (%)**	**TAW (cm/cm)**
Silt loam	0–30	1.43	18.10	31.70	7.93	23.77
	30–60	1.47	20.60	30.92	9.44	21.48
	60–90	1.52	21.23	29.87	10.14	19.89
	Average	1.47	19.98	30.83	9.17	21.71
Clay loam	0–30	1.40	18.54	38.88	25.44	13.44
	30–60	1.43	21.17	37.28	22.31	14.97
	60–90	1.45	22.36	36.56	21.98	15.01
	Average	1.43	20.69	37.57	23.24	14.47
Clay loam	0–30	1.39	23.81	41.56	28.38	13.44
	30–60	1.40	22.62	41.20	25.10	16.10
	60–90	1.43	19.85	40.65	25.02	16.56
	Average	1.41	22.09	41.14	26.17	15.37

P_d, bulk density in gmcm^{-3},Mc, Available soil moisture dry weight basis, %, FC- field capacity-%, PWP- permanent wilting point-%, TAW, total available water- cm/cm.

Water Practice & Technology Vol 16 No 3
doi: 10.2166/wpt.2021.033

The average water content at field capacity and permanent wilting point of the soil were determined to be 30.83 and 9.17%, respectively, for silt loam and 41.8 to 24.74 for clay loam. The moisture content at field capacity varied with depth between 31.7 to 30.9% and 37.28 to 41.56% on a mass basis for silt loam and clay loam, respectively. The top (0–30 cm) has a larger average water content of field capacity while the subsurface 30–90 cm has a lower value of field capacity in all textures.

The permanent wilting point moisture content showed variation with depth, as shown in Table 3. Total available water (TAW), which is the depth of water that a crop can extract from its root zone, is directly related to variation in field capacity and permanent wilting point. The total average available soil moisture for silt loam texture was 21.71 cm/cm and 14.47 to 15.37 cm/cm for clay loam. The measurement of infiltration rate at each sample site ranges between 10–15 mm hr^{-1} for silt loam and 5–7 mm/hr for clay loam soil using a double-ring infiltrometer. Hence, the average value of soil infiltration rate in the selected area of the study area was 12.0 and 6.0 mm hr^{-1} for silt clay and clay loam, which is analogous with WARC (2016).

Modeling and estimation of reference evapotranspiration

Reference crop evapotranspiration (ET_O) under current climate

Using the decadal averaged daily ET_O, reference evapotranspiration of the Shola Gebeya station is calculated by using the Penman-Monteith method, as shown in Table 4. It is observed that the annual reference crop evapotranspiration was estimated at 1,587.75 mm per year, which is equal to 43.5 mm per 10 days. The mean annual rainfall (1,114.12 mm per year) was lower than the reference crop evapotranspiration by 473.6 mm per year.

Table 4 | The monthly decadal (mm/dec) and daily (mm/day) average reference ETO at the selected area of study under the current climate (1984–2013)

	1st decade		2nd decade		3rd decade	
Month	**Per day**	**Decade**	**Per day**	**Decade**	**Per day**	**Decade**
Jan	3.77	37.70	3.16	31.60	3.92	39.20
Feb	4.19	41.90	3.65	36.50	4.88	48.80
Mar	4.87	48.70	4.12	41.20	4.94	49.40
Apr	4.80	48.00	4.12	41.20	4.72	47.20
May	4.86	48.60	4.06	40.60	5.21	52.10
Jun	4.37	43.70	3.86	38.60	4.60	46.00
Jul	3.34	33.40	3.47	34.70	3.43	34.30
Aug	3.70	37.00	3.81	38.10	3.88	38.80
Sep	4.30	43.00	3.98	39.80	4.41	44.10
Oct	4.55	45.50	3.72	37.20	4.54	45.40
Nov	4.14	41.40	3.25	32.50	4.04	40.40
Dec	3.73	37.30	2.92	29.20	3.87	38.70
Kiremt	3.93	39.28	3.78	37.80	4.08	40.80
Belg	4.68	46.80	4.24	42.40	4.94	49.38
Bega	4.05	40.48	3.99	39.90	4.09	40.93

Maximum ETO occurred in the month of March, which is 49.4 mm/dec, and the minimum occurred in the month of December, with a mean of 29.2 mm/dec.

Moreover, in the decade, maximum ETO was 52.10 mm, equivalent to 5.21 mm per day, and happened in the 3rd decade of May and the minimum value occurred during the 2nd decade of July which was estimated at 29.20 mm per decade. This implies that ET_O will be high during the *belg* seasons for

Water Practice & Technology Vol 16 No 3
doi: 10.2166/wpt.2021.033

the baseline period. This is due to high extreme temperature, wind and solar radiation, and low relative humidity. Therefore, the results imply that the enhancement of rainfall couldn't be a guarantee to reduce the rate of evapotranspiration. This is possibly due to the change in temperatures. In this regard, it was confirmed that climate change would have a severe consequence even in better rainfall distributions. Therefore, using this season for maize production would affect the yield in terms of water stress in the study area.

Modeling reference evapotranspiration using multiple variable regression

The constructed regression model takes the following form:

$$Y = -0.125 + 0.088 \times 1 + 0.008 \times 2 + 0.294 \times 3 + 0.324 \times 4 + 0.251 \times 5 - 0.016 \times 6 + 0.096$$

where: - Y is expected ETo, (**−0.125**) is an intercept of the variables, **0.096** is the standard error, x1, x2, x3, x4, x5, and x6 are Tmax, Tmin, Wind speed, Sunshine hour, Radiation, and Relative humidity respectively.

As shown in the model, Sunshine hour is the greatest contributor (at the rate of **0.324** unit), the second positively influencing variable is wind speed (**0.294** unit), the third positively influencing variable is solar radiation (**0.251** unit) followed by Tmax (**0.088** unit) and Tmin (**0.008** unit) (Table 5). Except for the relative humidity, which negatively influences by **−0.016** unit, other climate parameters had a positive effect on ETO. Positively influencing means occurred with increasing weather parameters, there could be an increase of ETO and vice versa for the negatively influencing variables. In agreement, Yadeta *et al.* (2020b) found that except for relative humidity, the remaining weather parameters have a direct relationship with ETO. Generally, the weather parameters used in the modeling and the specification formed were sufficient, implying that this model can be successfully used in estimating the ETO of the area, and another place having similar weather conditions with the study area.

Table 5 | Multiple linear regressions

Variable	Coefficients	Standard Error	t Stat	*P*-value	Lower 95%	Upper 95%
Intercept	−0.125	6.270	−0.02	0.985	−14.585	14.334
Tmax	0.088	0.196	0.446	0.667	−0.365	0.541
Tmin	0.008	0.065	0.12	0.906	−0.157	0.141
Wind speed	0.294	0.998	0.295	0.775	−2.007	2.595
Sunshine hour	0.324	0.259	1.25	0.246	−0.922	0.273
Radiation	0.251	0.110	2.273	0.053	−0.004	0.506
Relative humidity	−0.016	0.041	−0.40	0.696	−0.110	0.077

Analysis of variance (ANOVA) and regression model fitting for the predictors

94.8% of ETO variation shown has been caused by the joint influence of local weather parameters. Statistically, a realistic R^2 value was observed by the variance inflation factor and multiple regression model, which could be a sign of there being no multi-co-linearity problem among the selected predictor variables, as shown in Table 6. Validation results confirmed that the model with the used weather variables can effectively estimate the ETO of the study area, and areas with similar climatic conditions, with great performance. This result is also similar to Yadeta *et al.* (2020b).

Water Practice & Technology Vol 16 No 3
doi: 10.2166/wpt.2021.033

Table 6 | Regression model fitting for the predictors and ANOVA

Regression model	Regression value				
Multiple R	0.9852				
R square	0.9705				
Adjusted R square	0.9484				
Standard error	0.0959				
Observations	15				
Source	***df***	***SS***	***MS***	***F***	***P* value**
Regression	6	2.424	0.404	43.8975	1.080E-05
Residual	8	0.074	0.009		
Total	14	2.498			

R = coefficient of determination, R^2 = coefficient of multiple determination, R^2 = adjusted coefficient of multiple determination adjusted, df = degrees of freedom, SS = sum square, Ms = mean square, F = F-calculated, P-value = probability value.

Future reference crop evapotranspiration (ET_O)

The current study found that there is an expectation of high values of ET_O in future scenarios following the higher temperature. The ET_O in the baseline period, the 2020s and 2050s by scenarios are presented in Figure 3. Thus, ET_O in the base period varies in the range of 33.4 to 52.1 mm/dec. It increases roughly from 33.4 mm/dec in the 1st decade of July to the peak value of about 52.1 mm/dec in the 3rd decade of May. The highest ET_O in March can be explained by the hot (before the afternoon time) and windy weather conditions of this month.

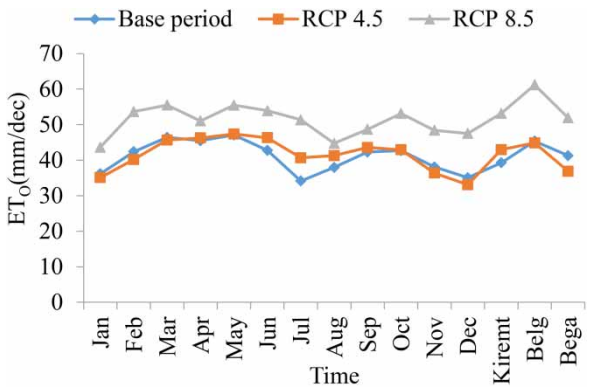

Figure 3 | Change in evapotranspiration (ET_O) by period and scenarios in the study area.

In the RCP 8.5 scenarios, minimum and maximum ET_O was predicted to be in the range of 44.3 to 75.3 mm/dec. In the 2nd decade of August, ET_O was minimal (44.3 mm/dec) while in the 1st decade of April ET_O was maximum (75.3 mm/dec). It increases roughly from about 44.3 mm/dec in the 2nd decade of August to the peak value of about 75.3 mm/dec in the 1st decade of April. In the case of RCP4.5 scenarios, ET_O varies in the range of 33 to 48 mm/dec. The ET_O increases roughly from approximately 33 mm/dec in the 1st decade of Dec to the peak value of about 48 mm/dec in the 3rd decade of May. The projected ET_O change between RCP 4.5 and RCP8.5 is significant (Figure 3).

Comparison between the base period and the scenarios show that the peak value ET_O increases from 33 to 48 mm/dec for RCP 4.5 and from 44.3 to 75.3 mm/dec for RCP 8.5. The yearly ten-day average ET_O was 40.88 mm/dec in the base period, which was predicted to be 41.57 mm/dec for RCP 4.5 and 58.44 mm/dec for RCP 8.5 scenarios. The percentile change in ET_O was found as

Water Practice & Technology Vol 16 No 3
doi: 10.2166/wpt.2021.033

−0.04, 1.02% for RCP 4.5 of the 2020s and 2050s and 21.24, 24.29% change in ETO for RCP 8.5 of the 2020s and 2050s respectively. The result is similar to the study undertaken by Rao *et al.* (2011).

The mean decadal change in ET_O for the two scenarios is presented by the period in Figures 4 and 5. These figures reveal that ET_O will be high during the *Belg* and *kiremt* seasons of the year. This is possibly due to the change in extreme temperatures. In this regard, it was confirmed that climate change would have a severe consequence even in better rainfall distributions (Yadeta *et al.* 2020a). *Kiremt* season will be characterized by the lower rate of reference evapotranspiration in both 2020s and 2050s for the two scenarios in respect of *belg* season.

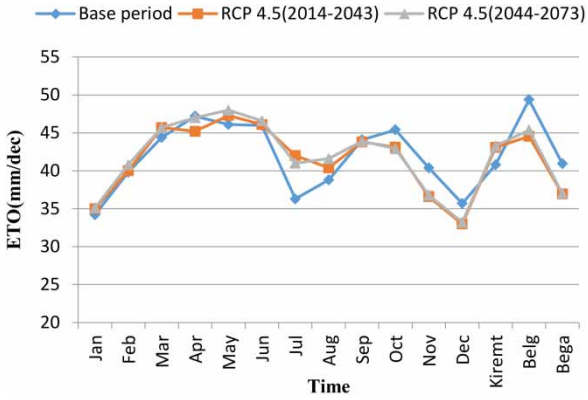

Figure 4 | The ten-day change pattern of ET_O at the study area by period for the RCP 4.5 scenario.

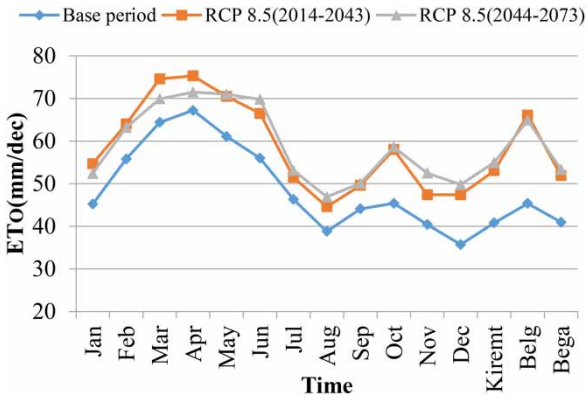

Figure 5 | The ten-day change pattern of ET_O at the study area by period for the RCP 8.5 scenario.

Effective rainfall under the influence of variable climate scenarios

As per the USDA S.C (1985) method, the effective rainfall was calculated for each growing period and stage of maize as shown below on a monthly basis for the baseline period (Table 7).

Like that of the baseline period, the effective rainfall of the future period was calculated via the USDA S.C (1985) method, for each growing period and stage of maize as shown below on a monthly basis (Table 8).

Adjusting crop characteristics based on the observed climatic conditions

The suggested values of k_c for maize growth by FAO-56 guidelines are 0.15 for initial, 1.5 for mid-season, and 0.5 for late-season. However, during the baseline period, the relative humidity is between

Water Practice & Technology Vol 16 No 3
doi: 10.2166/wpt.2021.033

Table 7 | The monthly basis recorded and effective rainfall (mm/month) for the baseline period

Months	Rec. rain (mm)	Eff. rain (mm)
Jan	19.10	18.50
Feb	14.80	14.40
March	61.60	55.60
Apr	109.70	90.40
May	216.80	141.60
Jun	83.30	72.20
Jul	327.40	157.70
Aug	318.60	156.90
Sep	85.80	74.00
Oct	15.0	14.60
Nov	12.80	12.50
Dec	8.70	8.60

Rec. rain – recorded rainfall; Eff. Rain – effective rainfall.

Table 8 | The monthly basis recorded and effective rainfall (mm/month) for the future period under the two scenarios for near-century

	RCP 4.5 (a)		RCP 4.5 (b)		RCP 8.5 (c)		RCP 8.5 (d)	
Month	Est. rain	Eff. rain	Est. rain	Eff. rain	Est. rain	Eff. rain	Est. rain	Eff. rain
Jan	54.3	49.6	54.3	49.6	24.6	23.6	51.8	47.5
Feb	47.2	43.6	29.5	28.1	26.8	25.7	20.3	19.7
March	43.2	40.2	16.8	16.4	46.3	42.9	33.6	31.8
Apr	106.5	88.4	37.0	34.8	59.6	53.9	63.6	57.2
May	209.5	139.3	84.8	73.3	169.2	123.4	164.0	121
Jun	126.3	100.8	184.0	129.8	97.5	82.3	123.9	99.4
Jul	274.7	152.5	126.7	101.0	294.5	154.5	325.0	157.5
Aug	278.9	152.9	316.5	156.6	263.8	151.4	315.4	156.5
Sep	67.8	60.5	309.2	155.9	61.1	55.1	65.4	58.6
Oct	11.1	10.9	68.2	60.7	12.5	12.3	13.8	13.5
Nov	6.8	6.7	14.1	13.8	12.8	12.5	16.1	15.7
Dec	4.1	4.1	10.4	10.2	1.4	1.4	3.8	3.7

Est., estimated rainfall, mm, Eff., effective rainfall, mm; RCP 4.5: (a) 2020s; (b) 2050s, RCP 8.5: (c) 2020s; (d) 2050s.

50 and 80% and wind speed is greater than 2 m/s in the months of June, July, August, and September. Hence, the k_c value was adjusted as per Equations (14) for mid-season, as shown in Table 9.

Table 9 | The suggested and adjusted kc and growth stage value for each growth stage of the maize growing period

Crop stage	Suggested K_c	Computed K_c	Suggested growth stage	Comp. growth stage
Initial	0.15	0.15	20	18
Mid-season	1.50	1.51	35	31
Late season	0.50	0.50	30	26

During the initial stage for annual crops, evapotranspiration is mostly in the form of evaporation. Therefore, precise estimates for $K_{c\ ini}$ were considered the frequency with which the soil surface is wetted during the initial period. Where the soil is frequently wet from rain, the evaporation from

Water Practice & Technology Vol 16 No 3
doi: 10.2166/wpt.2021.033

the soil surface can be considerable and $K_{c\ ini}$ is large. On the other hand, when the soil surface is dry, evaporation is restricted and the $K_{c\ ini}$ are small (Table 9). $K_{c\ mid}$ is less affected by wetting frequency than is $K_{c\ ini}$, as vegetation during this period is generally near full ground cover so the effects of surface evaporation on K_c are lesser. For frequent rain of crops, the $K_{c\ mid}$ of less than 1.0, the value can be replaced by approximately 1.1–1.3 to account for the combined effects of continuously wet soil (FAO 2011). Therefore, both the soil surface and vegetation are dry and the value for the $K_{c\ end}$ was relatively small.

Regarding depletion fraction, the suggested depletion fraction by FAO was 0.55% for $ET_O \approx 5$. But the average ET_O during the maize growing period in the Berehet woreda was 4.06 mm/day, which is less than the suggested one. Hence, the depletion fraction during the maize production period needs adjustment using Equation (9). As per the equation, the adjusted value of depletion fraction in percentage was adjusted to 0.59%.

Estimation of maize and irrigation water requirement under the influence of variable climate scenarios

Maize crop evapotranspiration (ETc) of the baseline period

Often rainfall is vital but not adequate to cover the water requirement of the crops (Smith *et al.* 2006). Crop production in the dry season is only possible with irrigation, while it might be possible in the rainy season but unreliable because of prolonged dry spells and drought; yields will be less than optimal production. When rainfall is not enough to cover the water demands of crops, irrigation water has to supplement the rainwater in such a way that the rain and irrigation water together satisfies the water needs of crops.

It is essential to know the water requirement of a crop, which is the total quantity of water required from its sowing time up to harvest. Different crops may have different water requirements at different places in the same country, depending upon the climate, type of soil, method of cultivation, and effective rain. At the same time, water supplies available for irrigation will become more variable and will decline because of climate variability and change. Climate alteration will affect agriculture by boosting water demand, off-putting crop productivity, and dropping water availability in areas where irrigation is most needed or has a comparative advantage.

Thus, once climate change impacts are appraised, it is important to analyze what measures should be taken to adapt to the potential consequences of climate variability related to irrigation. One possibility is to expand irrigation with locally available water sources. Where rain-fed cropping systems are displaced to the margins, the delivery of irrigation plays a strategic role in either stabilizing the production of grains or in supporting a low danger, high-value production system with a strong commercial focus.

Therefore, the water needs of maize crops during the baseline period were done for clay loam soil textures since it covers more than 70% of the selected area. Table 10 shows summaries of crop water and irrigation needs of maize in the study area. A maize variety with a growing period of 110 days to maturity would require 403.2 mm depth of water, while 67 mm would be required as supplementary irrigation depth.

Implication of climate change on maize water needs under future period

As per the baseline period, maize water needs for the future period under RCP 4.5 and RCP 8.5 scenarios need input data like ET_O, soil data, crop data, and effective rainfall for computation of maize water needs. Even though it is recommended to estimate future soil data, its value varies between pointed intervals (FAO 2011). Therefore, soil data of the baseline period were used for the future one, and the above determined ET_O, crop data and effective rainfall were used.

Water Practice & Technology Vol 16 No 3
doi: 10.2166/wpt.2021.033

Table 10 | Summary for total water and irrigation requirements for maize under the baseline period (1984–2013)

Month	Decade	Stage	Kc	ETc (mm/day)	ETc (mm/dec)	Eff rain (mm/dec.)	Irr. Req. (mm/dec)
Jun	1	Init	0.15	0.72	7.2	2.7	0.7
Jun	2	Init	0.15	0.68	6.8	16.7	0.0
Jun	3	Dev	0.17	0.72	7.2	28.7	0.0
Jul	1	Dev	0.48	1.73	17.3	45.8	0.0
Jul	2	Dev	0.86	2.73	27.3	56.7	0.0
Jul	3	Dev	1.26	4.28	47.0	55.2	0.0
Aug	1	Mid	1.49	5.47	54.7	55.0	0.0
Aug	2	Mid	1.49	5.69	56.9	56.1	0.8
Aug	3	Mid	1.49	6.01	66.1	45.6	20.4
Sep	1	Late	1.32	5.62	56.2	33.1	23.0
Sep	2	Late	0.96	4.26	42.6	23.6	19.1
Sep	3	Late	0.65	2.9	20.3	12.1	2.9
Total					403.2	431.4	67.0

Accordingly, the crop water and irrigation requirements of a maize variety with a growing period of 110 days to maturity were predicted to be 436.1 and 445.1 mm depth of water during the 2020s and 2050s of the future period for RCP 4.5, while 101.8 to 63.7 mm depth of water would be required as supplementary irrigation respectively. Whereas, 441.3 and 447.3 mm depth of water was required during the 2020s and 2050s of the future period for RCP8.5, while 142.9 to 134.0 mm would be required as supplementary irrigation for both periods of RCP 8.5 scenarios (Table 11).

These results reveal that the average rate of CWR is increased approximately by 8.16 and 10.39% for RCP 4.5 and by 9.45 and 10.94% for RCP 8.5 scenarios of the 2020s and 2050s respectively. The result is similar to the study undertaken by Rao *et al.* (2011). According to Rao *et al.* (2011), the crop water requirement of maize for the future period of 2025 and 2050 ranges between 404 to 447 mm in semi-humid to semi-arid agro-ecology from the base period of the 1990s. Also, it is significant to note that projections of water demands of semi-humid to arid for the future period, which is worked out by the IWMI (International Water Management Institute), said that even with the lower estimates projected by the IWMI, there will be a substantial future increase in irrigation water requirements (Sharma 2006).

CONCLUSION

This study quantifies climate change impacts on crop and irrigation water demand in the middle Awash River basin. The main rainy season (*Kiremt*) starts at 156 DOY for the baseline period and 161 to 171 DOY for RCP 4.5 of the 2020s and 2050s and 168 and 173 DOY for RCP 8.5 of the 2020s and 2050s of a future period. It ceases in the range of 274 to 286 DOY for the baseline and future periods and has an LPG of between 113 to 118 rainfall days. In this season, the rain will likely increase by about 1.8% by the 2020s and 20% by the 2050s for RCP 4.5 and 6% by the 2020s, and 21.73 by the 2050s for RCP 8.5 scenarios.

ETO is in the range of 33.4 to 52.1 mm per decade in the base periods, which is predicted to be in the range of 44.1 to 75.3, and 33 to 77.3 mm per decade for RCP 4.5 and RCP 8.5 respectively for the 2020s and 2050s. Overall, there is 0.04, 1.02% for RCP 4.5 of the 2020s and 2050s, and 21.2, 24.3% change in ETO for RCP 8.5 of the 2020s and 2050s from the base period. CWR will be 436.1, 445.1 mm for RCP 4.5 and 441.3, 447.3 mm for RCP 8.5 and IR ranges between 63.7 to 101.8 mm for RCP 4.5 and 142.9 to 134 mm for RCP 8.5 of the 2020s and 2050s. CWR will increase by 5.1 and 9.5% for RCP 4.5 and by 6.55 and 10.3% for RCP 8.5 of the 2020s and 2050s from the base

Water Practice & Technology Vol 16 No 3
doi: 10.2166/wpt.2021.033

Table 11 | Summary for total water and irrigation requirements for maize under future climate: 2014–2043 (a); 2044–2073 (b)

		Kc coeff		ETc (mm/day)		ETc (mm/dec)		Eff rain (mm/dec.)		Irr. Req. (mm/dec)	
(a) Month	Decade	4.5(a)	4.5(b)	4.5(a)	4.5(b)	4.5(a)	4.5(b)	4.5(a)	4.5(b)	4.5(a)	4.5(b)
Jun	2	0.13	0.13	0.82	0.82	8.20	8.20	29.30	47.30	0.00	0.00
Jun	3	0.14	0.14	0.80	0.80	8.00	8.00	36.50	42.80	0.00	0.00
Jul	1	0.40	0.40	1.97	1.97	19.70	19.70	46.70	34.20	0.00	0.00
Jul	2	0.76	0.76	3.26	3.26	32.60	32.60	53.20	29.70	0.00	2.90
Jul	3	1.14	1.14	4.95	4.95	54.40	54.40	52.50	37.20	1.90	17.20
Aug	1	1.39	1.41	6.20	6.20	62.00	65.00	53.80	47.80	8.20	14.20
Aug	2	1.39	1.41	6.21	6.21	62.10	64.10	55.40	54.90	6.70	9.20
Aug	3	1.39	1.42	6.26	6.26	68.90	70.90	43.60	53.90	25.20	15.00
Sep	1	1.26	1.26	5.71	5.71	57.10	58.10	29.10	55.00	28.10	2.10
Sep	2	0.90	0.89	4.11	4.11	41.10	41.10	18.10	56.40	22.90	3.00
Sep	3	0.57	0.60	2.76	2.76	22.00	23.00	10.60	35.50	8.70	0.00
Total						436.10	445.10	428.90	494.70	101.80	63.70
		Kc coeff		ETc (mm/day)		ETc (mm/dec)		Eff rain mm/dec)		Irr. Req. (mm/dec)	
(b) Month	Decade	8.5(a)	8.5(b)	8.5(a)	8.5(b)	8.5(a)	8.5(b)	8.5(a)	8.5(b)	8.5(a)	8.5(b)
Jun	2	0.14	0.14	0.89	0.89	2.70	2.70	6.60	8.80	2.70	2.70
Jun	3	0.14	0.14	0.81	0.81	8.10	8.10	31.90	37.10	0.00	0.00
Jul	1	0.18	0.18	1.01	1.01	10.10	10.10	45.80	47.90	0.00	0.00
Jul	2	0.51	0.51	2.46	2.46	24.60	24.60	55.00	55.30	0.00	0.00
Jul	3	0.88	0.89	4.13	4.13	45.40	45.40	53.50	54.30	0.00	0.00
Aug	1	1.29	1.28	5.59	5.59	55.90	55.90	53.70	55.40	2.20	0.60
Aug	2	1.45	1.48	5.81	5.81	58.10	60.10	54.90	56.80	3.30	1.40
Aug	3	1.47	1.48	6.03	6.03	66.30	67.30	42.70	44.40	23.60	22.00
Sep	1	1.47	1.47	6.27	6.27	62.70	62.70	27.40	28.70	35.30	34.00
Sep	2	1.15	1.15	5.35	5.35	53.50	53.50	15.90	17.00	37.70	36.50
Sep	3	0.81	0.79	3.95	3.95	39.50	39.50	11.90	12.80	27.60	26.70
Oct	1	0.54	0.55	2.87	2.87	14.30	17.30	3.80	4.00	10.60	10.30
Total						441.30	447.30	403.20	422.50	142.90	134.00

period. Increment in CWR can cause an increase in stress on the water resource. In this study, a new ETO model is developed using a multiple variable linear regression model and its degree of fitting is statistically tested and Kc is adjusted for the local climate; hence, it can be used in future irrigation and related studies. Generally, decision-makers, farmers, irrigation engineers, and other stakeholders can use the results of this study in irrigation design, monitoring, scheduling, and other related activities. Further studies on climate modeling that integrate soil-water-atmosphere, socio-economic and institutional aspects of a climate system under different emission scenarios by using multiple crop simulation models should be conducted to assess the potential impact of future climate change on crop production and design adaptation strategies for development policy for the future.

ACKNOWLEDGEMENTS

Special thanks are due to the Ethiopian National Meteorological Agency for providing us with the meteorological data. Also, we would like to acknowledge the Werer Agricultural Research Centre soil laboratory for analyzing the physicochemical properties of soil.

Water Practice & Technology Vol 16 No 3
doi: 10.2166/wpt.2021.033

DISCLOSURE STATEMENT

The authors declare no conflict of interest.

DATA AVAILABILITY STATEMENT

All relevant data are included in the paper or its Supplementary Information.

REFERENCES

Abiy, G., Shoeb, Q. & Girma, M. 2014 Analysis of seasonal rainfall variability for agricultural water resource management in Southern Region, Ethiopia. *Journal of Natural Sciences Research* **4** (11), 2014.

Allen, R. G., Pereira, L. S., Raes, D. & Smith, M. 1998 *Crop Evapotranspiration: Guideline for Computing Crop Water Requirements*. FAO No 56. Food and Agriculture Organization, Water Resources, Development and Management Service, Rome, Italy.

Allen, R. G., Dirk, R. & Martin, S. 2005 *Crop Evapotranspiration (Guidelines for Computing Crop Water Requirements) FAO Irrigation and Drainage Paper No. 56*. FAO, Water Resources, Development and Management Service Rome, Italy. Available from: http://www.fao.org/docrep/X0490E/X0490E00.htm.

Andreadis, K. M. & Letten Maier, D. P. 2006 Trends in 20th-century drought over the continental United States. *Geophys. Res. Lett.* **33**, L10403.

Carter, T. R. 1996 Assessing climate change adaptations: the IPCC Guidelines. In: *Adapting to Climate Change: An International Perspective* (Smith, J. B., ed.). University College London, London, UK. pp. 27–43.

Carter, M. R. & Gregorich, E. G. 1993 Soil sampling and methods of analysis, 2nd edn (M. R. Carter & E. G. Gregorich, eds). Canadian Society of Soil Science, Pinawa, Manitoba. ISBN (13): 978-0-8493-3586-0, pp.1891–1894.

Cutforth, H. W., McGinn, S. M., McPhee, E. & Miller, P. R. 2007 Adaptation of pulse crops to the changing climate of the Northern Great Plains. *Agron. J.* **99**, 1684–1699.

Djaman, K., O'Neill, M., Owen, C. K., Smeal, D., Koudahe, K., West, M., Allen, S., Lombard, K. & Irmak, S. 2018 Crop evapotranspiration, irrigation water requirement and water productivity of maize from meteorological data under semiarid climate. *Water* **10**, 405.

FAO (Food and Agricultural Organization) 2011 *Facts, Perspectives, Impacts, and Actions Required in the 21st Century: Ensuring Food Security in A Changing World*. Background paper prepared for the High-Level Conference on World Food Security: The challenges of climate change and bioenergy, FAO, Rome, Italy.

FAO (Food and Agricultural Organization) 2012 *Digital Soil Map of the World and Derived Soil Properties (CDROM)*. Food and Agriculture Organization of the United Nations, (FAO), Rome, Italy.

Gan, T. Y. 2000 Reducing vulnerability of water resources of Canadian Prairies to potential droughts and possible climate warming. *Water Resour. Manag.* **14**, 111–135.

Gebrehiwot, T. & van der Veen, A. 2013 Assessing the evidence of climate variability in the northern part of Ethiopia. *J. Dev. Agric. Econ.* **5**, 104119.

Gebremeskel, G. & Kebede, A. 2017 Spatial estimation of long-term seasonal and annual groundwater resources: application of WetSpass model in the Weriiwatershed of the Tekeze River Basin, Ethiopia. *Phys. Geogr.* **38**, 338e359.

Ghamarnia, H., Jafarizade, M., Meri, E. & Gobadei, M. A. 2013 Lysimetric determination of *Coriandrum sativum* L. water requirement and single and dual crop coefficients in a semiarid climate. *J. Irrig. Drain. Eng.* **139**, 447–455.

Green, G. C. 1966 *The Evaluation of Methods of Rainfall Analyses and the Application to the Rainfall Series of Nelspruit*. MSc thesis *(Agro-meteorology)*. University of the Orange Free State, Bloemfontein, South Africa, pp. 147.

IPCC 2007 *New Assessment Methods and the Characterization of Future Conditions: In Climate Change 2007: Impacts, Adaptation, and Vulnerability*. Contribution of working group II to the fourth assessment report of the Intergovernmental Panel on climate change. Cambridge University Press, Cambridge, UK, pp. 976.

IPCC 2013 In: *The Physical Science Basis. Contribution of Working Group I to the Fifth Assessment Report on IPCC* (Stocker, T. F., Qin, D., Plattner, G.-K., Tignor, M., Allen, S. K., Boschung, J., eds). Cambridge University Press, Cambridge, United Kingdom, p. 1535, and New York, NY, USA.

Kim, S. T. & Yu, J. Y. 2012 The two types of ENSO in CMIP5 models. *Geophys. Res. Lett.* **39** (11).

Kim, U., Jagath, J. K. & Vladimir, U. S. 2008 Generation of monthly precipitation under climate change for the upper Blue Nile river basin, Ethiopia. *J. Am. WaterResour. Assoc.* **44**, 12321247.

Ko, J., Piccinni, G. & Steglich, E. 2009 Using EPIC model to manage irrigated cotton and maize. *Agric. Water Manag.* **96**, 1323–1331.

LADA 2008 *Guidelines for Land Use System Mapping; Technical Report*. FAO, Rome, Italy.

OECD 2013 *The Climate Challenge: Achieving Zero Emissions*. Available from: http://www.oecd.org/env/the-climatechallenge-achieving-zero-emissions.htm (accessed on 10 August 2020).

Water Practice & Technology Vol 16 No 3
doi: 10.2166/wpt.2021.033

Osborne, C. P., Chuine, I., Viner, D. & Woodward, F. I. 2000 Olive phenology as a sensitive indicator of future climatic warming in the Mediterranean. *Plant Cell Environ.* **23**, 701–720.

Osima, S. 2018 Projected climate over the greater horn of Africa under 1.5°C and 2°C global warming. *Environ. Res. Lett.* 13, 065004.

Paeth, H., Kaib, O., Ralf, P. & Daniela, J. 2005 Regional dynamical downscaling over West Africa: model evaluation and comparison of wet and dry years. *Meteorol.Z.* **14**, 349e367. Raghunath, H.M., 20.

Parry, M., Arnell, N., Hulme, M., Nicholls, R. & Livermore, M. 1998 Adapting to the inevitable. *Nature* **395**, 741.

Quiroga, S. & Iglesias, A. 2009 A comparison of the climate risks of cereal, citrus, grapevine, and olive production in Spain. *Agric. Syst.* **101**, 91–100.

Rao, V. U. M., Rao, A. V. M. S., Rao, G. G. S. N. & Satyanarayana, T. 2011 *Impact of Climate Change on Crop Water Requirements and Adaptation Strategies*, pp. 311–319. https://doi.org/10.1007/978-3-642-19360-6.

Richter, G. M. & Semenov, M. A. 2005 Modelling impacts of climate change on wheat yields in England and Wales: assessing drought risks. *Agricultural Systems* **84**(1), 77–97.

Saad, A. M. A., Shari_, N. M. & Gairola, S. 2011 Nature and causes of land degradation and desertification in Libya: need for sustainable land management. *Afr. J. Biotechnol.* **10**, 13680–13687.

Sahlemedin, S. & Taye, B. 2000 *Procedures for Soil and Plant Analysis*. National Soil Research Center Ethiopian Agricultural Research Organization, Technical Addis Ababa, Ethiopia, p. 74.

Sharma, B. R. 2006 *Crop Water Requirements and Water Productivity: Concepts and Practices*. Groundwater governance in Asia. Available from: http://www.waterandfood.org/gga/Lecture20%Material/B.R.Sharma_CWR&WP.pdf.

Smith, M., Kivumbi, D. & Heng, L. K. 2006 *Use of the FAO CROPWAT Model in Deficit Irrigation Studies*. Water Report No. 22, FAO (Food and Agriculture Organization), Rome, Italy.

Stern, R., Knock, J., Rijks, D. & Dale, I. 2003 *INSTAT Climatic Guide*, pp. 398. Available from: http://www.reading.ac.uk/ssc/software/instat/climatic.pdf.

Stern, R., Rijks, D., Dale, I. & Knock, J. 2006 INSTAT climatic guide. Statistical Services Centre, The University of Reading, Reading, UK, p. 230.

Subramanya, K. 2008 *Engineering Hydrology*, 3rd edn. Tata McGraw Hill, New Delhi, India, pp. 155–162.

Tekleab, S., Mohamed, Y. & Uhlen Brook, S. 2013 Hydro-climatic trends in the Abay /Upper Blue Nile basin, Ethiopia. *Physics and Chemistry of the Earth* **61–62**, 32–42.

Tessema, N., Kebede, A. & Yadeta, D. 2020 Modelling the effects of climate change on streamflow using climate and hydrological models: the case of the Kesem sub-basin of the Awash River basin Ethiopia. *Int J River Basin Manag.* https://doi.org/10.1080/15715124.2020.1755301.

UNEP 2000 *Sourcebook of Alternative Technologies for Freshwater Augmentation in West Asia*. Available from: http://www.unep.or.jp (accessed on 10 August 2020).

USDA-SCS 1985 *National Engineering Handbook, Section 4-Hydrology*. USDA-SCS, Washington, DC.

Wang, X., Cai, D., Wu, H., Hoogmoed, W. B. & Oenema, O. 2016 Effects of variation in rainfall on rainfed crop yields and water use in dryland farming areas in China. *Arid Land Res. Manag.* **30**, 1–24.

WARC (Werer Agricultural Research Centre) 2016 *The Annual Research Report*. Werer, Ethiopia.

Weller, E. & Cai, W. 2013 The realism of the Indian ocean dipole inCMIP5 models: the implications for climate projections. *J. Clim.* **26**, 6649–6659.

White, R. P. & Nackoney, J. 2003 *Drylands, People, and Ecosystem Goods and Services: AWeb-Based Geospatial Analysis*. Available from: http://pdf.wri.org/drylands.pdf (accessed on 10 August 2020).

Willmott, C. J. & Kenji, M. 2005 Advantages of the mean absolute error (MAE) over the root mean square error (RMSE) in assessing average model performance. *Clim. Res*. 30, 7982.

Yadeta, D., Kebede, A. & Tessema, N. 2020a Climate change posed agricultural drought and potential of the rainy season for effective agricultural water management, Kesem sub-basin, Awash Basin, Ethiopia. *Theoretical and Applied Climatology* **139**(3–4). https://doi.org/10.1007/s00704-020-03113-7.

Yadeta, D., Kebede, A. & Tessema, N. 2020b Potential evapotranspiration models evaluation, modelling, and projection under climate scenarios, Kesem sub-basin, Awash River basin, Ethiopia. *Modeling Earth Systems and Environment* **6**. https://doi.org /10.1007/s40808-020-00831-9.

First received 4 January 2021; accepted in revised form 22 March 2021. Available online 30 March 2021